

Kinetics Studies of Sintered Nepheline Syenite Alkaline Leaching under Atmospheric Pressure

Kianmehr Mohammadloo¹ · Shima Barakan¹ · Somayeh Shayanfar¹ · Valeh Aghazadeh¹

Received: 18 March 2021 / Accepted: 11 May 2021 / Published online: 9 June 2021
© The Indian Institute of Metals - IIM 2021

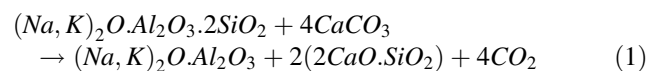
Abstract The purpose of this study is to develop the kinetic model and to find the optimum leaching conditions for maximum alumina dissolution from sintered nepheline syenite resource in the alkaline solution. About 80% of alumina (smaller than 5% of silica) was effectively recovered at 80 °C, 3 M NaOH, particle size less than 88 μm, agitation speed of 800 rpm, and leaching time of 60 min with a minimum amount of silica dissolution. Based on the kinetic model and the obtained reaction degree of each effective parameter, the experimental data were simulated. The simulation results proved that the leaching process for alumina was controlled by diffusion through the solid product layer and reaction at the interface of unreacted core that was confirmed by the value of activation energy (15.53 kJ/mol). The provided optimum conditions could be effective to decrease the silica dissolution, and to improve the alumina recovery.

Keywords Sintered nepheline syenite · Alkaline leaching · kinetics · Alumina dissolution · Silica dissolution

1 Introduction

Alumina has shown a widespread application in electronics industry, chemical, oil and gas processing, wear-resistant parts, and so on [1]. To produce alumina, bauxites are the dominant Al-bearing resource. However, the lack of high-grade bauxites in some countries has received much

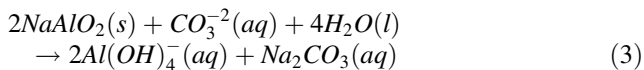
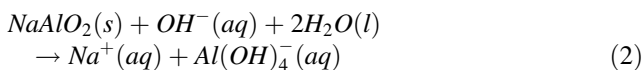
attention to alternative alumina resources [2]. Nepheline syenite, an anhydrous sodium potassium alumina silicate, is one of the alumina non-bauxite resources which have been historically exploited [3, 4]. Nepheline syenite shows more efficiency in ore processing for alumina production in the point of view of low operating cost, low environmental pollution, and the production of by-products such as sodium and potassium carbonates [5]. Alumina can be extracted either by acid leaching & thermal activation [6], or alkaline solution leaching & lime mixture sintering [7–9]. Acidic leaching is not a suitable method for alumina extraction from nepheline syenite resources in contrast to clay and fly ash resources. In this method, the production of silica gel imposes some problems in the filtration process and high amounts of impurities enter into the leaching solution during further processing steps [8]. Alumina production process from nepheline syenite is mainly composed of sintering, alkaline leaching, desilication, carbonation, and calcination [10]. On the pressurized alkaline leaching, high energy leaching agent have been consumed by using NaOH in the autoclave at the temperature of 150–250 °C [11]. Therefore, in this study, the alkaline leaching was carried out at the atmospheric pressure. In the leaching process, the alumina of nepheline syenite was converted to sodium and potassium aluminates (soluble compounds in alkaline solvent) and the silica was transformed to dicalcium silicate (insoluble compounds in alkaline solvent). This process is conducted by Eq. (1) [5]:



The reactions between sodium aluminate and leaching agent, NaOH or Na₂CO₃, are shown as Eqs. (2) and (3) [5].

✉ Valeh Aghazadeh
v.aghazadeh@sut.ac.ir

¹ Department of Mineral Processing, Faculty of Mining Engineering, Sahand University of Technology, Tabriz, Iran



Since the high-quality alumina production is initially obtained by controlling its leaching condition, the targeted alkaline leaching is a suitable hydrometallurgical method for dissolving alumina from sintered nepheline syenite. Therefore, in the present study, the important parameters such as leaching agent concentration, leaching time, temperature, particle size, and agitation speed are studied to obtain a solution containing high Al_2O_3 dissolution (i.e., with a little loss of Al_2O_3 and minimum dissolution of SiO_2).

This present paper showed a comprehensive study about the kinetic investigation of Al and Si dissolution after a leaching process. In this research, the kinetic model was applied to demonstrate the leaching mechanism through the investigation of the physicochemical condition of the leaching process. The determination of Si dissolution behavior in the kinetic study could be effective to find the optimum conditions for minimum Si dissolution in alkaline leaching. In this research, the experimental results were also simulated by the kinetic models to find the meaningful relationship between the real and simulated data to reach the maximum alumina recovery yield.

2 Material and Methods

2.1 Material

Sintered Nepheline syenite was obtained from Azarshahr alumina pilot plant located in Eastern Azerbaijan Province, Iran. All chemical materials were purchased from Merck Co., Germany.

2.2 Experimental Procedures

The leaching experiment was carried out at a 2L glass reactor equipped with a water-cooled condenser. The bottle cap and mechanical mixer were used to suspend all fine particles of nepheline syenite by varying the type of impellers and the agitation speeds. Each experiment was done by pouring 1L of leaching agent into the reactor. It was heated in the temperature ranges from 20 to 80 °C by using a thermostatically controlled water bath (± 0.1 °C). Then, 150 g of sintered nepheline syenite was added to the leaching agents. During the leaching process, some samples were collected to analyze the aluminum (Al) and silica (Si) concentrations. After the leaching process of sintered

nepheline syenite, the slurry was quickly filtered and the desilication process was performed. Figure 1 shows the flowsheet of leaching and the other processes for alumina production from sintered nepheline syenite. The concentrations of Al and Si were measured by atomic absorption spectroscopy and UV–Visible spectrophotometer, respectively. To characterize the leaching residue, X-ray powder diffraction (XRD), X-ray fluorescence analysis (XRF), scanning electron microscope, and energy dispersive spectrometer (SEM–EDS) were also used.

2.3 Kinetic Models

The kinetics study plays an essential role to explain the mechanism of the leaching process of sintered nepheline syenite using NaOH and Na_2CO_3 solution by evaluating the kinetic model with the experimental data. The shrinking core model is the most important kinetic model to describe the leaching process of metal ions [12–21]. The shrinking core model indicates that the leaching process is controlled by the diffusion of reactant through the solution boundary layer and may be controlled through a solid product layer or by the rate of the surface chemical reaction. The equations of reactions were controlled by chemical reaction and diffusion calculated from Eqs. (4) and (5), respectively [6]:

$$1 - (1 - X)^{\frac{1}{3}} = k_r t \quad (4)$$

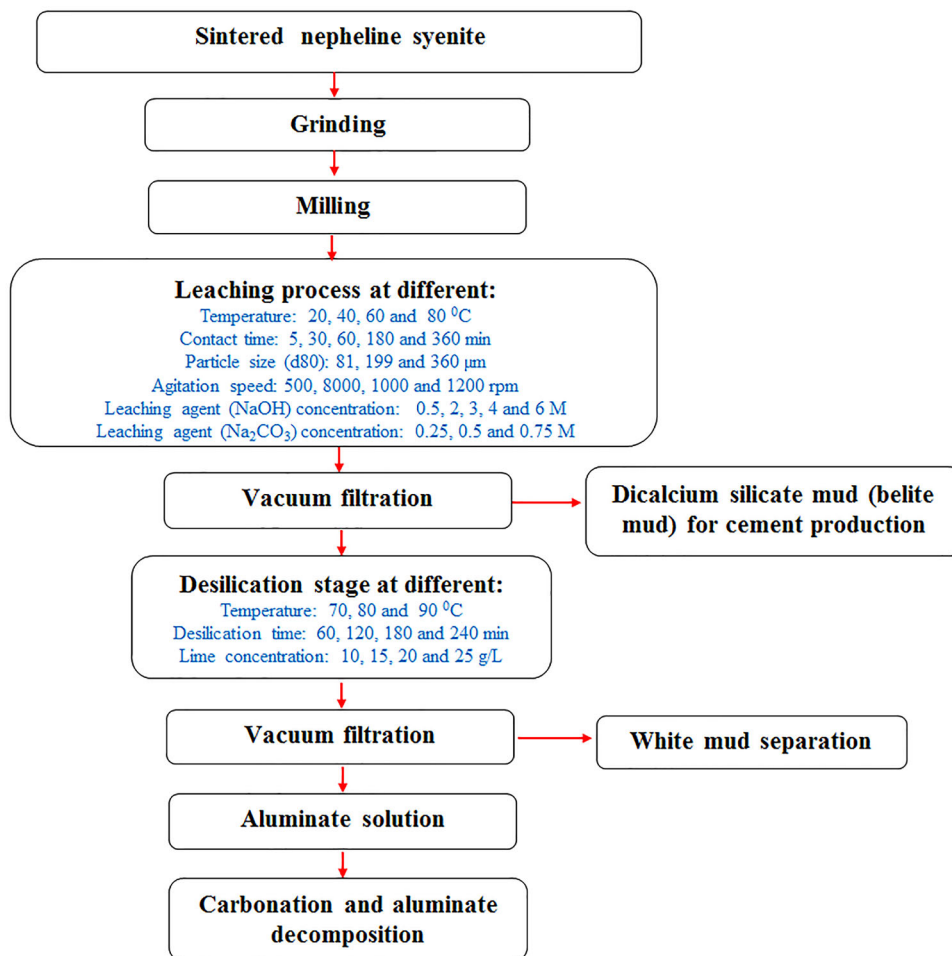
$$1 - \left(\frac{2}{3}\right)X - (1 - X)^{\frac{2}{3}} = k_d t \quad (5)$$

where X is the fraction reaction after time (t), k_d and k_r are the kinetics constants for diffusion and chemical reaction control, respectively. In Eq. (6), it is assumed that in addition to diffusion from reaction product layers, the reaction can be controlled through the interface of unreacted core and the layer composed of reaction products [22].

$$\frac{1}{3} \ln(1 - X) - 1 + (1 - X)^{-\frac{1}{3}} = \frac{2bD_e C_A}{\rho_s r_0^2} = k_d t \quad (6)$$

D_e is the molecular weight of dissolving metal, C_A , r_0 , b , ρ_s are the concentration of the dissolved lixiviant A in the bulk solution, the initial radius of the solid particle, the diffusion coefficient in the porous product layer, and the stoichiometric coefficient of the reagent in the leaching reaction, respectively. Equation (3) reveals that if the surface reaction controls the rate, the relation between the left side of the equation and time must be linear. The slope of this line is called the apparent rate constant which is directly proportional to $1/r_0$ [23]. If the diffusion through the product layer controls the leaching rate, there must be a linear relationship between the left side of Eq. (5) and time.

Fig. 1 Flowsheet for hydrothermal beneficiation process of sintered nepheline syenite to produce alumina



The slope of the line is an apparent rate constant and it must be directly proportional to $1/r_0^2$ [24]. The temperature dependence of the reaction rate constant can be calculated by Arrhenius equation (Eq. 7) ²⁵:

$$k = A \exp\left(-\frac{E_a}{RT}\right) \tag{7}$$

where A is the frequency factor, E_a is the activation energy of the reaction, R is the universal gas constant, and T is the absolute temperature [7]. In this way, the values less than 20 kJ/mol indicate diffusion-controlled processes, while the high values of activation energy greater than 40 kJ/mol mention the chemical reaction control [26–28].

3 Results and Discussion

3.1 Physicochemical Characterizations of Sintered Nepheline Syenite

The initial grain size of the sintered nepheline syenite is relatively large in the range of 6–12 cm. Therefore, these raw materials were ground by using a laboratory jaw crusher and ball mill. Sieve analysis was used to determine the particle size distribution of the ground sample. As shown in Fig. 2a to c, the ground sintered nepheline syenite were separated into three particle size fractions.

The chemical composition of the initial sintered nepheline syenite sample was determined by XRF and listed in Table 1. The mineralogical composition and chemical phases of this sample were identified by XRD in Fig. 3. The obtained results indicated that the sintered nepheline syenite mainly contained dicalcium silicate (Larnite), sodium aluminate, and calcium sodium aluminate. Therefore, the sintering process was efficient to form

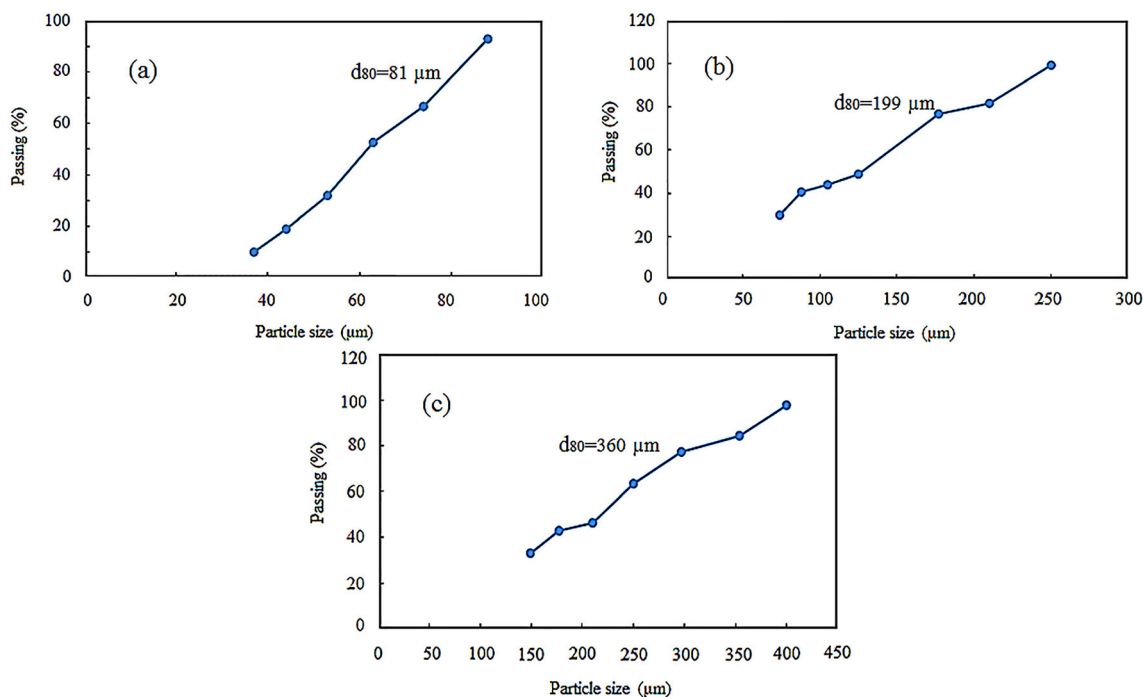


Fig. 2 The particle size fractions of ground sintered nepheline syenite **a** from 38 to 88 μm , **b** from 88 to 250 μm , and **c** from 210 to 400 μm

Table 1 XRF analysis of sintered nepheline syenite fed to the leaching process

| Component | SiO ₂ | Al ₂ O ₃ | K ₂ O | Na ₂ O | CaO | MgO | Fe ₂ O ₃ | MnO | P ₂ O ₅ | SO ₃ | TiO ₂ | L.O.I |
|----------------|------------------|--------------------------------|------------------|-------------------|-------|------|--------------------------------|--------|-------------------------------|-----------------|------------------|-------|
| Amount (% wt.) | 24.57 | 8.94 | 4.37 | 2.57 | 50.10 | 0.57 | 3.80 | < 0.10 | 0.17 | < 0.10 | 0.30 | 4.60 |

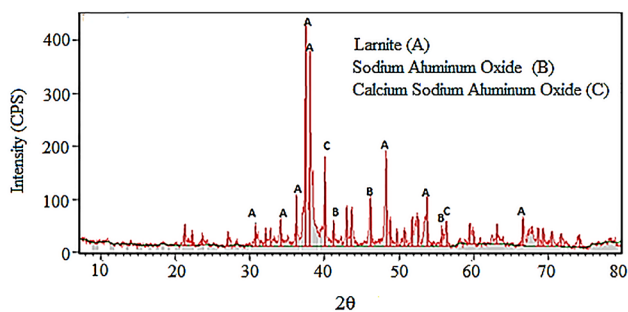


Fig. 3 XRD analysis of sintered nepheline syenite fed to the leaching process

aluminate salts soluble in alkaline solution in the leaching process, and the formation of dicalcium silicate with low solubility in alkaline solution.

3.2 Effect of Different Leaching Conditions

In this study, the alkaline leaching efficiency of sintered nepheline syenite was investigated to find the optimum processing parameters. Accordingly, the effect of various

leaching agents such as NaOH and Na₂CO₃ in different concentrations, temperature, particle size, and contact time were evaluated. Figure 4a to h shows the dissolution behavior of Al and Si from alkaline leaching of sintered nepheline syenite under different conditions.

As shown in Fig. 4a and b, the increase in the concentrations of leaching agents (NaOH or NaOH + Na₂CO₃) significantly enhanced the Al₂O₃ recovery in less than 60 min. According to Fig. 4c and d, the increase of temperature and decrease of particle size also improved the dissolution of alumina due to the increase of the probability of collision between particles.

The influence of leaching conditions on silica dissolution behavior is illustrated in Fig. 4e to h. According to these results, the increase of NaOH leaching agent concentration was obtained to be less than 10% of silica dissolution during 60 min. However, the synergistic effect of both NaOH and Na₂CO₃ leaching agents increased the silica dissolution. As shown in Fig. 4g, increasing the temperature from 20 to 80 °C made a low increase in the silica dissolution. With decreasing the particle size (Fig. 4h) from 400 to 88 μm , the silica dissolution was also

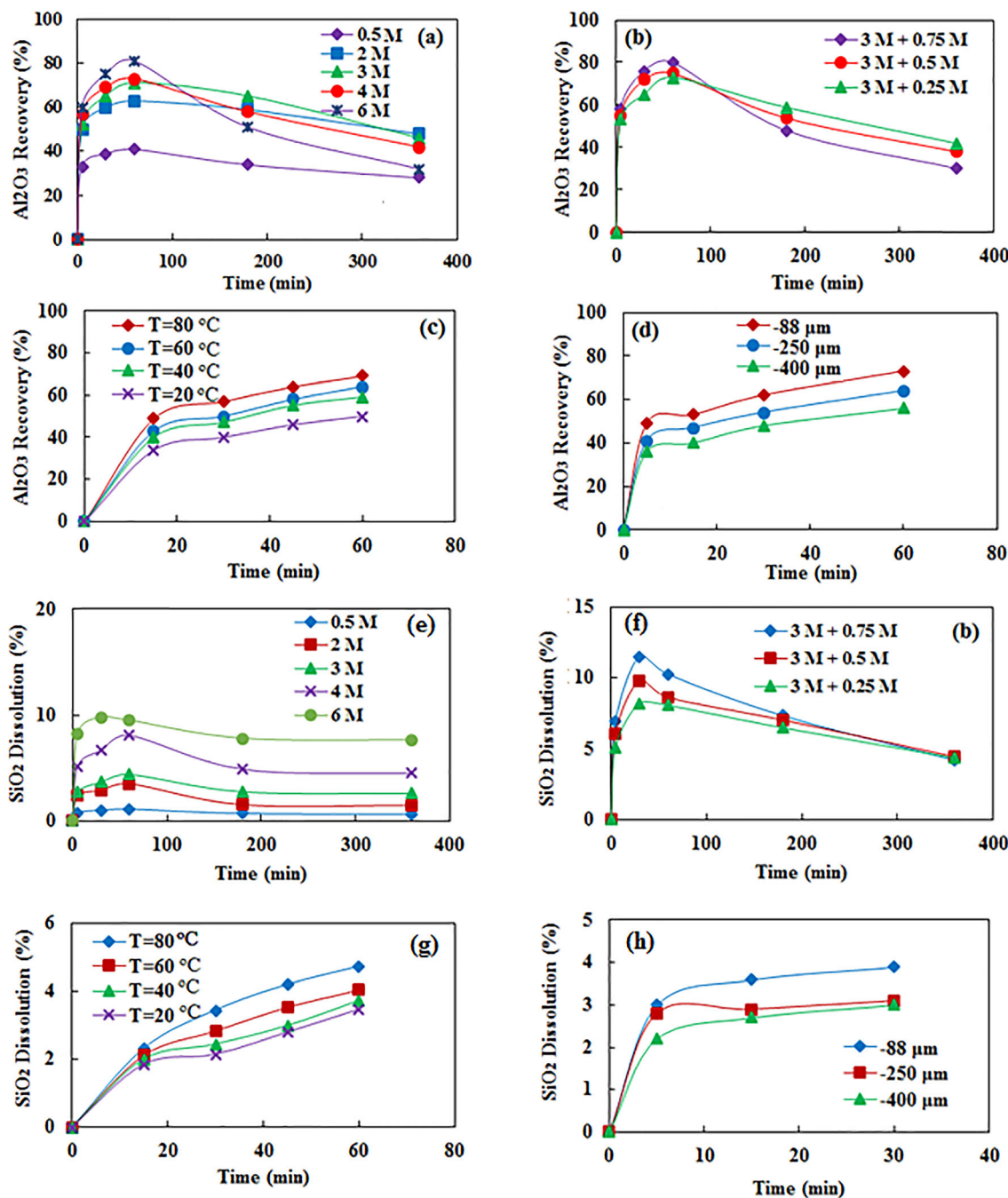
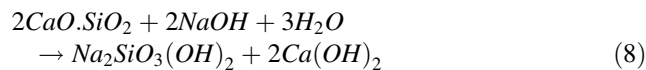


Fig. 4 The alumina and silica dissolution under consideration of NaOH concentration (a) and (e); NaOH + Na₂CO₃ concentration (b) and (f), temperature (c) and (g), and particle size (d) and (h), respectively, by sample uptaking at different times

changed slightly. Therefore, with regard to the leaching results, the optimum conditions for getting maximum Al₂O₃ recovery (up to 80%) and minimum silica dissolution were obtained at temperature = 80 °C, NaOH concentration = 3 M, agitation speed = 800 rpm, particle size less than 88 μm, and leaching time = 60 min.

In all experiments, the Si and Al leaching decreased in the solution after 60 min which might be explained by the

formation of dicalcium silicate and its reaction with NaOH to produce Na₂SiO₃(OH)₂ (Eq. (8)).



Furthermore, Ca(OH)₂ could react to sodium aluminate in the solution to produce calcium hydroaluminates (CaAl₂O₄·6H₂O) according to Ea. (9):

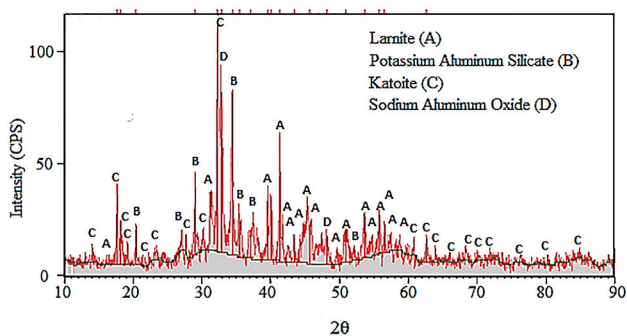
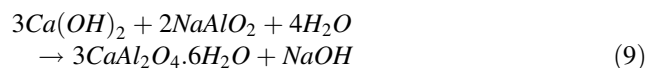
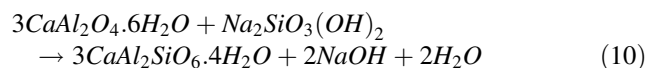


Fig. 5 The XRD analysis of belite mud

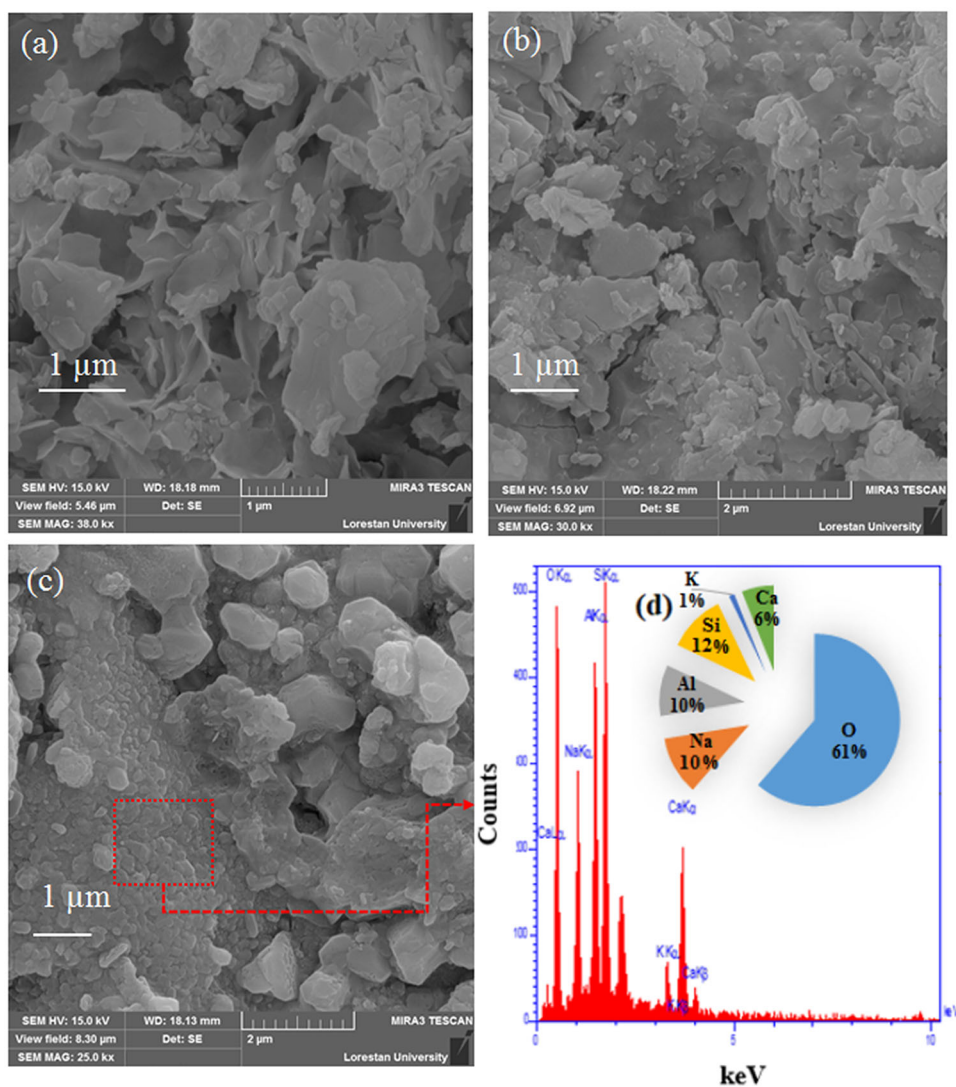


In this condition, calcium hydroaluminates was unstable and reacted to $Na_2SiO_3(OH)_2$ to produce calcium hydroalumosilicate (Eq. 10).



The precipitation of calcium hydroalumosilicate on the surface of nepheline syenite particles formed the passive layer and inhibited the access of leaching agents to the internal structure of the materials. So the Al and Si concentrations decreased in the solution after 60 min.

Fig. 6 SEM micrograph of **a** sintered nepheline syenite before leaching, **b** belite mud after 60 min alkaline leaching, **c** belite mud after 360 min alkaline leaching, and **d** EDS analysis of belite mud surface after 360 min alkaline leaching



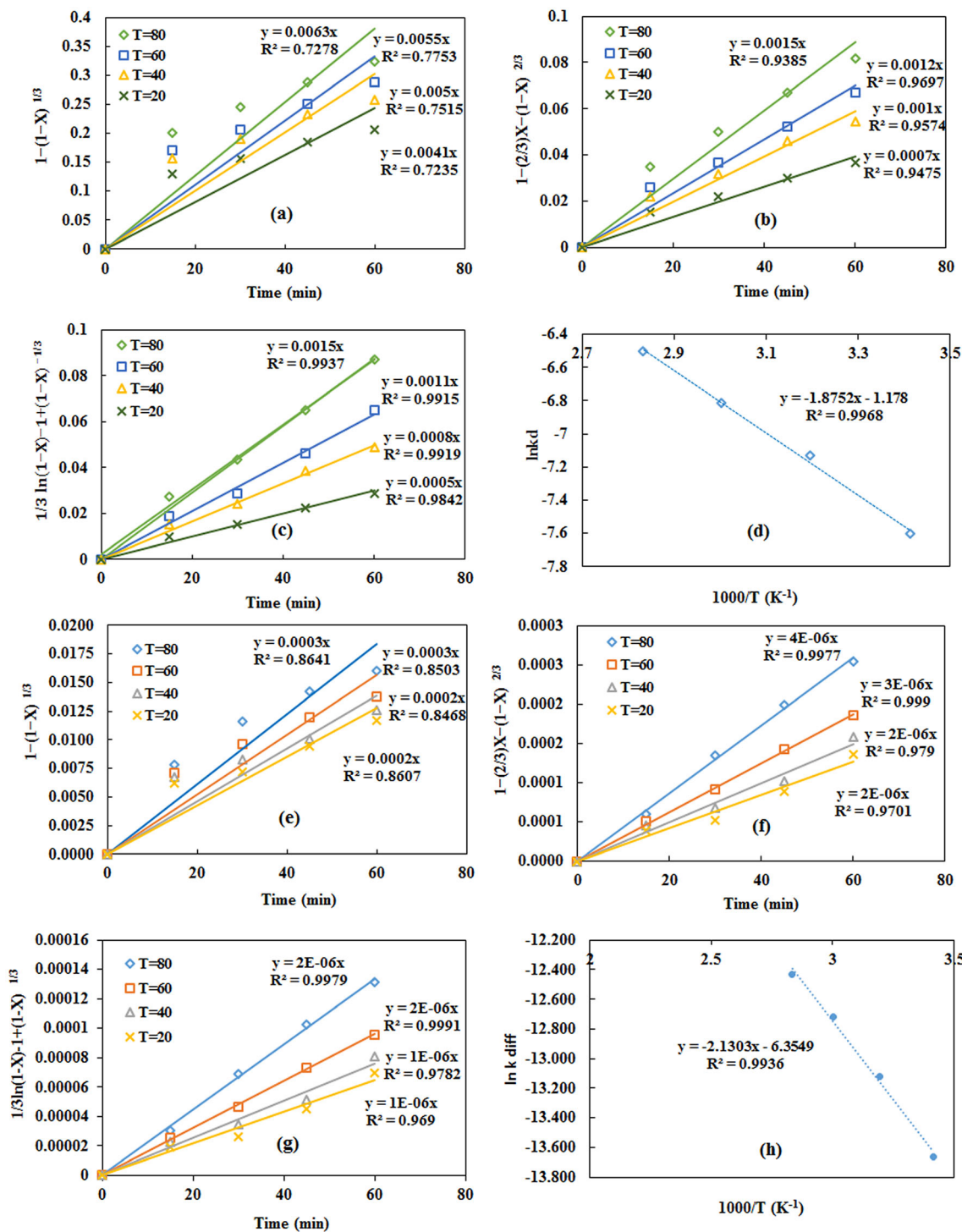


Fig. 7 Kinetic plots of alumina and silica dissolution based on surface chemical reaction (a) and (e); diffusion of the product layer (b) and (f), diffusion control from the layer formed from products and interface of unreacted core models (c) and (g) at 3 M NaOH, 60 min, 800 rpm, and particle size less than 88 μm, and the Arrhenius plot (d) and (h), respectively

The XRD analysis of leaching residue (belite mud) is shown in Fig. 5. Obtained results indicated the presence of dicalcium silicate (Larnite), calcium hydroalumosilicate (Katoite), and sodium and potassium hydroalumosilicates.

Accordingly, it seems that the leaching process under 3 M NaOH concentration, at 80 °C, 60 min, 800 rpm, and the particle size less than 88 μm was suitable to dissolve alumina and to prepare insoluble silica compounds.

Table 2 The amount of $\ln k_d$ at different temperatures

| Temperature (°C) | T (k) | 1000/T | k_d | $\ln k_d$ |
|------------------|-------|--------|--------|-----------|
| 20 | 293 | 3.41 | 0.0005 | -7.60 |
| 40 | 313 | 3.19 | 0.0008 | -7.13 |
| 60 | 333 | 3.00 | 0.0011 | -6.81 |
| 80 | 353 | 2.83 | 0.0015 | -6.50 |

The morphologies of the sintered nepheline syenite and the belite mud are examined in Fig. 6a to c. These results agreed well with the leaching experiment data to form a passive layer after 60 min. Figure 6c illustrated the complete coating of belite mud surface with the passive layer after 360 min leaching. According to EDS data in Fig. 6d, this passive layer consisted of calcium and sodium hydroalumosilicate which decreased alumina recovery in the solution after 60 min.

3.3 Kinetic Study

The curves of kinetic models related to chemical control, diffusion control through the layer on the product surface, and diffusion control from the layer formed from products are depicted in Fig. 7a, b and c, respectively. As shown in Fig. 7c, the results of calculated kinetic models showed good compliance with the product layer diffusion and reaction at the surface of the unreacted core model. For this model, the value of correlation coefficients (R^2) was closer to 1. Therefore, the apparent rate constant k_d was extracted from the slope of Fig. 7c equation, which was directly presented in Table 2. The rate constants could be used for determining the temperature dependency by Arrhenius' law to calculate the activation energy.

Figure 7d shows the plot of activation energy with the amount of 15.53 kJ/mol. Since the calculated activation energy was lower than 20 kJ/mol, the leaching process fitted well with the controlling model of diffusion through the product layer and reaction at the surface of the unreacted core.

During leaching of nepheline syenite, in addition to alumina dissolution, dissolved silica could also enter into the solution. Therefore, the kinetics of silica dissolution should be investigated. The graphs of the kinetic models based on Eqs. (3), (4) and (5) are shown in Figs. 7e, f and g, respectively. Based on these results, the correlation coefficient related to diffusion control was close to 1 and the diffusion through the product layer controlled the leaching process. Figure 7h shows the plot of activation energy with the calculated amount of 15.87 kJ/mol. This activation energy value showed the diffusion controlling step.

According to this kinetic result, the possible mechanism for silica diffusion in alkaline leaching was the decomposition of dicalcium silicate precipitation.

As shown in Fig. 8a to h, the selected kinetic models for both alumina and silica dissolution were investigated to find the degree of reaction of effective parameters such as particle size fraction (r_0), agitation speed (rpm), and the concentration of $[\text{OH}^-]$ & $[\text{CO}_3^{2-}]$ related to NaOH & Na_2CO_3 leaching agents. In this way, k_d could be extracted from the slopes of Fig. 8a to h. Therefore, the degree of reaction was determined by plotting the $\ln k_d$ versus $\ln r_0$, $\ln(\text{rpm})$, $\ln [\text{OH}^-]$, and $\ln [\text{CO}_3^{2-}]$.

As shown in Fig. 9a to h, the obtained slope for each parameter reflected the degree of reaction. Accordingly, Eq. (11) represented the leaching kinetics of sintered nepheline syenite for maximum alumina dissolution. Based on Eq. (12), the leaching kinetics of silica was also determined.

$$\begin{aligned} \frac{1}{3} \ln(1 - X) - 1 + (1 - X)^{-\frac{1}{3}} &= k_d t \\ &= 3.353 [\text{OH}^-]^{1.05} [\text{CO}_3^{2-}]^{0.43} r_0^{-0.63} (\text{rpm})^{0.94} \exp\left(-\frac{15.53}{RT}\right) t \end{aligned} \quad (11)$$

$$\begin{aligned} 1 - \left(\frac{2}{3}\right)X - (1 - X)^{\frac{2}{3}} \\ &= k_d t = 4.16 [\text{OH}^-]^{0.000004} [\text{CO}_3^{2-}]^{0.00003} r_0^{-0.32} (\text{rpm})^{0.00001} \\ &\exp\left(-\frac{15.87}{RT}\right) t \end{aligned} \quad (12)$$

These results showed that the increase of agitation speed, the concentration of $[\text{OH}^-]$ & $[\text{CO}_3^{2-}]$, and the decrease of particle size improved the alumina dissolution with a small amount of silica in alkaline solution during the leaching process. By plotting the left and right sides of Eqs. (11) and (12) in Fig. 10, the correlation coefficient of 0.9 indicated a strong positive correlation between the test data and those predicted by Eq. (11).

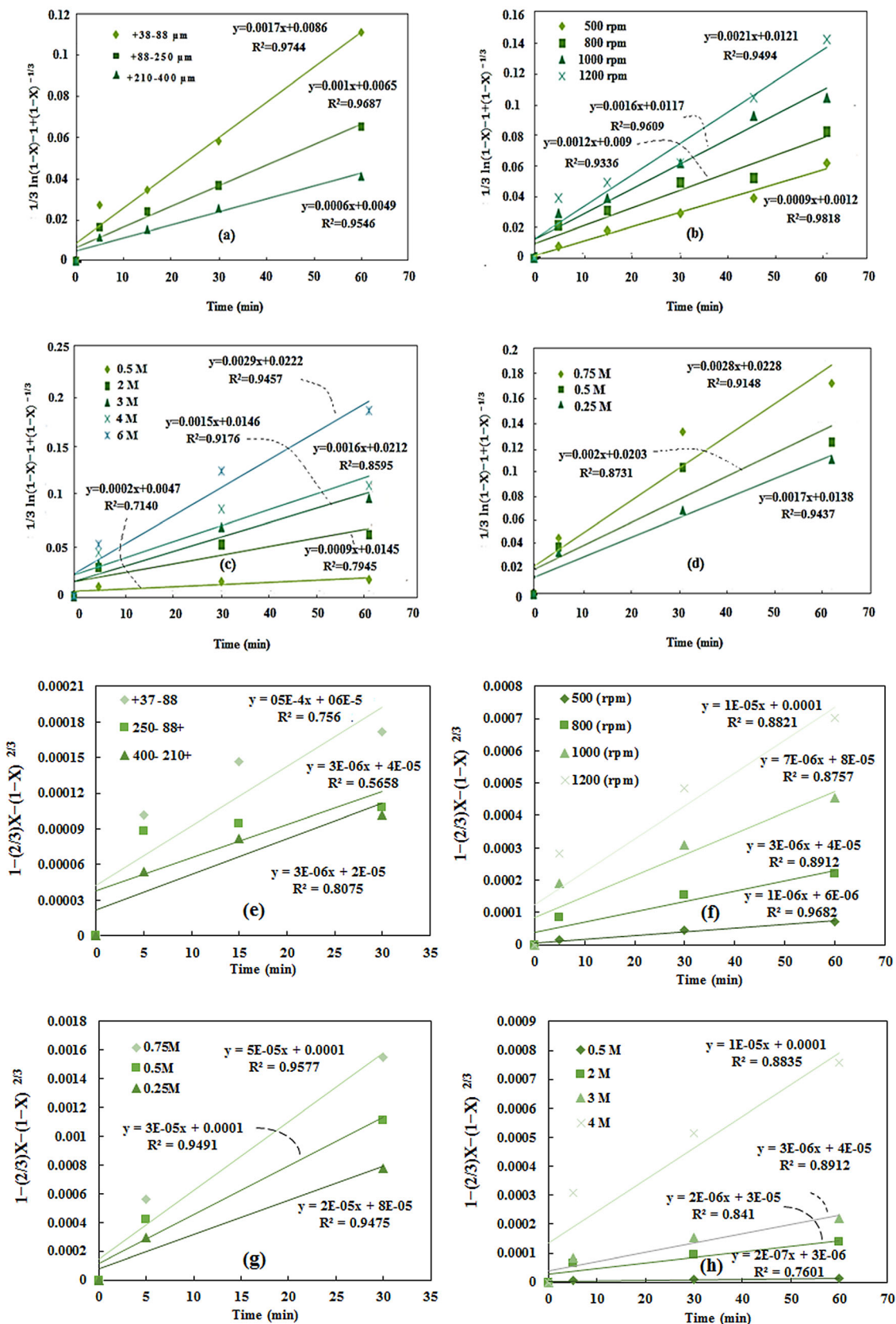


Fig. 8 Kinetic plots of effective parameters on alumina and silica dissolution particle size fraction (a) and (e); agitation speed (b) and (f); the concentration of $[OH^-]$ (c) and (g); and the concentration of $[CO_3^{2-}]$ (d) and (h), respectively

Fig. 9 Plots for alumina and silica dissolution based on $\ln k_d$ vs $\ln(\text{rpm})$ (a) and (e); $\ln r_0$ (b) and (f); $\ln [\text{OH}^-]$ (c) and (g), and $\ln [\text{CO}_3^{2-}]$ (d) and (h)

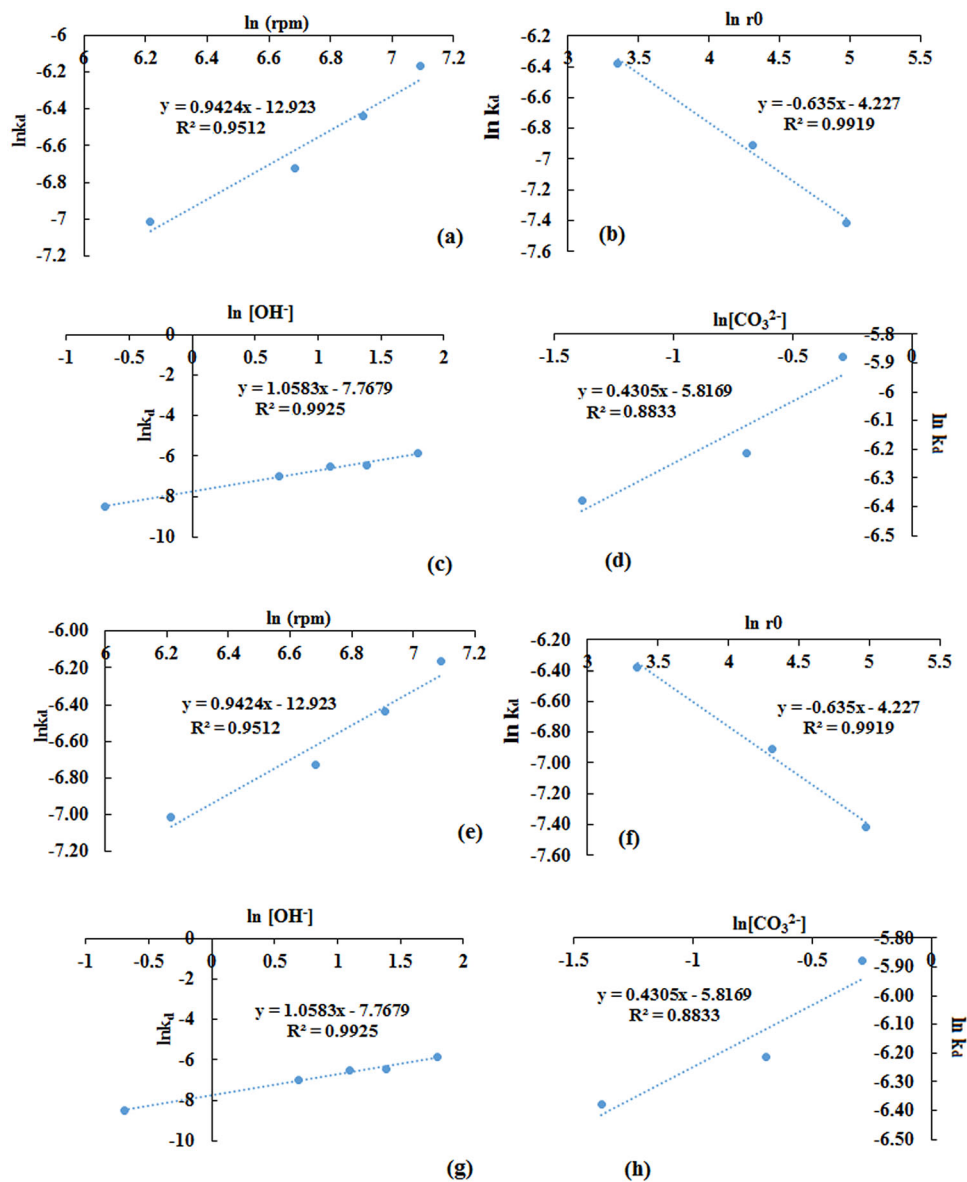
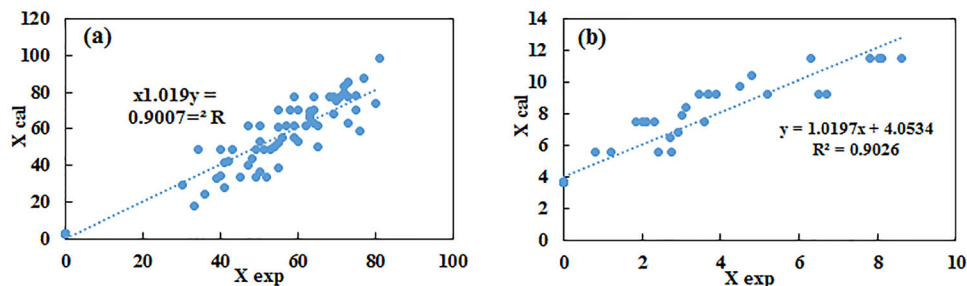


Fig. 10 Comparison of experimental and calculated data of sintered nepheline syenite dissolution in the alkaline leaching solution for **a** alumina dissolution and **b** silica dissolution



4 Conclusions

According to the experimental results, the optimum conditions for maximum alumina recovery (with minimum silica dissolution) were achieved at 80 °C, NaOH

concentration of 3 M, during 60 min, particle size less than 88 μm , and agitation speed of 800 rpm.

Contact time played a critical role in the leaching process. Based on the SEM-EDS and XRD analysis data, the formation of the passive layer after 60 min leaching

(optimum contact time) extensively reduced the dissolution of alumina.

In this research, the experimental data were also used to evaluate the shrinking core kinetic models. Simulation results represented that the shrinking core model could illustrate the real phenomenon of the leaching process. The activation energy values related to alumina production and silica dissolution were calculated as 15.53 and 15.87 kJ/mol, respectively. It was proven that the alkaline dissolution of the sintered nepheline syenite was controlled by the diffusion through the product layer and reaction at the interface of the unreacted core for alumina dissolution, and the diffusion of the product layer for silica dissolution. Therefore, by understanding the leaching mechanism and the degree of reaction of effective parameters, the maximum dissolution rate of alumina (up to 80%) was achieved.

Acknowledgements The authors acknowledge the support of Iranian Mines & Mining Industries Development & Renovation (IMIDRO) with grant number of 494/7087 for providing financial support to carry out this research.

Author Contributions Authors 1: Kianmehr Mohammadloo Designed and performed experiments, collected data, and analyzed the data. Authors 2: Shima Barakan Wrote the paper, collected research, and managed the data. Authors 3: Somayeh Shayanfar Performed experiments and analyzed the data. Authors 4: Valeh Aghazadeh. Supervisor, co-wrote the paper and investigated research. All authors read and approved the final manuscript.

Funding Iranian mines and mining industries development and renovation (IMIDRO) with Grant Number of 494/7087.

Declarations

Conflict of interest The authors declare that they have no competing interests.

Availability of Data and Materials The authors confirm that the data supporting the findings of this study are available.

Code Availability There is not any used codes in this research.

References

- [1] 1. P. B. Parikh, *Transactions of the Indian Ceramic Society*, 1995, **54**(5), 179-184.
- [2] 2. T. S. Barry, T. Uysal, M. Birinci, and M. Erdemoğlu, *Mining, Metallurgy & Exploration*, 2019, **36**(3), 557-569.
- [3] 3. S. Vinogradov and V. Sizyakov, *Metallurgist*, 2009, **53**(3-4), 242-247.
- [4] A. Panov, S. Vinogradov, and S. Engalychev 'Evolutional development of alkaline aluminosilicates processing technology', In 'Light Metals 2017', 9-16; 2017, Springer.
- [5] 5. B. Arlyuk and A. Pivnev: 'Efficiency of nepheline ore processing for alumina production', in 'Essential Readings in Light Metals', 983-997; 2016, Springer.
- [6] A. A. Al-Zahrani, *Engineering Sciences*, 2009, **20**(2).
- [7] 7. Z. Yao, M. Xia, P. Sarker, and T. Chen, *Fuel*, 2014, **120**, 74-85.
- [8] 8. A. R. Nizami, *J. Chem. Soc. Pak*, 2012, **34**(3), 570.
- [9] 9. J. P. Hamilton, S. L. Brantley, C. G. Pantano, L. J. Criscenti, and J. D. Kubicki, *Geochimica et Cosmochimica Acta*, 2001, **65**(21), 3683-3702.
- [10] Y. Estrin, M. Y. Murashkin, and R. Valiev, *Processing and Applications*, 2010, 468
- [11] 11. V. Kazakov, V. Lipin, V. Matveev, D. Maiorov, and V. Korovin, *Russian Journal of Applied Chemistry*, 2013, **86**(1), 1-5.
- [12] 12. X.-l. Feng, Z.-q. Long, D.-l. Cui, L.-s. Wang, X.-w. Huang, and G.-c. Zhang, *Transactions of Nonferrous Metals Society of China*, 2013, **23**(3), 849-854.
- [13] 13. Y. Wang, S. Jin, Y. Lv, Y. Zhang, and H. Su, *Minerals*, 2017, **7**(2), 27.
- [14] 14. J. Huang, M. Chen, H. Chen, S. Chen, and Q. Sun, *Waste management*, 2014, **34**(2), 483-488.
- [15] 15. L. Popovič, P. Raschman, J. Spišák, A. Fedoročková, and G. Sučík, *Hydrometallurgy*, 2020, **196**, 105441.
- [16] 16. R.-c. Wang, Y.-c. Zhai, and Z.-q. Ning, *International Journal of Minerals, Metallurgy, and Materials*, 2014, **21**(2), 144-149.
- [17] 17. U. Sultana, F. Gulshan, M. Gafur, and A. Kurny, *American Journal of Materials Engineering and Technology*, 2013, **1**(3), 30-34.
- [18] A. L. A. Santos, E. M. A. Becheleni, P. R. M. Viana, R. M. Papini, F. P. C. Silvas, and S. D. F. Rocha, *Mining, Metallurgy & Exploration*, 2020.
- [19] 19. W. Astuti, T. Hirajima, K. Sasaki, and N. Okibe, *Mining, Metallurgy & Exploration*, 2015, **32**(3), 176-185.
- [20] 20. R. K. Nadirov, *Transactions of the Indian Institute of Metals*, 2019, **72**(3), 603-607.
- [21] 21. B. Mojtahedi, S. Rasouli, and H. Yoozbashizadeh, *Transactions of the Indian Institute of Metals*, 2020, **73**(4), 975-987.
- [22] 22. C. Dickinson and G. Heal, *Thermochimica Acta*, 1999, **340**, 89-103.
- [23] C. A. Young, P. R. Taylor, and C. G. Anderson: 'Hydrometallurgy 2008: Proceedings of the Sixth International Symposium'; 2008, SME.
- [24] 24. A. Itodo, I. Eneji, B. Mnenga, and M. Tseen, *Academic Journal Chemistry*, 2019, **4**(9), 69-80.
- [25] P. Rahimi Borujerdi, B. Shotorban, S. Mahalingam, and D. R. Weise, *International Journal of Heat and Mass Transfer*, 2019, **145**, 118672.
- [26] 26. S. He, T. Peng, H. Sun, D. Luo, Q. Xiao, and Q. Geng, *Open Chemistry*, 2019, **17**(1), 1146-1156.
- [27] 27. W.-N. Mu, Y.-C. Zhai, and L. Yan, *Transactions of Nonferrous Metals Society of China*, 2010, **20**, s87-s91.
- [28] 28. F. M. Santos, P. S. Pina, R. Porcaro, V. A. Oliveira, C. A. Silva, and V. A. Leão, *Hydrometallurgy*, 2010, **102**(1-4), 43-49.

Publisher's Note Springer Nature remains neutral with regard to jurisdictional claims in published maps and institutional affiliations.